Using Derivatives to Compare Cortical Waves Across Preparations

KAY A. ROBBINS
Department of Computer Science and Cajal Neuroscience Research Center,
The University of Texas at San Antonio, 6900 N. Loop 1604 West, San Antonio, Texas 78249
krobbins@cs.utsa.edu

DAVID M. SENSEMAN
Department of Biology and Cajal Neuroscience Research Center,
The University of Texas at San Antonio, 6900 N. Loop 1604 West, San Antonio, Texas 78249
senseman@utsa.edu

Abstract. Visual stimulation evokes waves of depolarization that propagate within and between cytoarchitectually distinct cortical areas in the turtle. These waves appear to reflect underlying low-dimensional characteristics that can be captured using Karhunen-Loéve (KL) decomposition. The KL analysis produces spatial basis functions with modal characteristics. However, while the qualitative structure of these spatial modes is similar across preparations, the details vary with the specific geometric and constituent characteristics of each preparation. This paper develops a technique for comparing derivative-response relationships across preparations. We verify that these derivative-response relationships hold for *in vivo*, *in vitro* and simulated preparations of the turtle cortex.

Keywords: cortical waves, KL decomposition, derivative-response

1. Introduction

In turtles, visual stimulation evokes a complex wave of depolarization within the cerebral cortex (Prechtl, 1994; Prechtl et al., 1997; Senseman, 1996, 1999). The wave originates in the rostral pole of the dorsal cortical area (D) which receives a direct afferent projection from the lateral geniculate complex of the thalamus. Waves evoked by visual stimulation propagate at a relatively uniform velocity of 0.01–0.04 m/s from the rostral pole into the caudal pole of dorsal cortex. However, the wave also travels dorsomedially into a secondary visual area, the dorsomedial cortex (DM). As the advancing wave front crosses the cortical boundary and enters DM it slows significantly. Waves with the same qualitative features have been observed in *in vitro* (Senseman, 1996, 1999; Senseman and Robbins, 1999, 2002) and *in vivo* preparations (Prechtl, 1994; Prechtl et al., 1997, 2000) as well as for model simulations (Nenadic et al., 2000, 2002a, 2002b). The goal of the current study is to compare certain structural features of the waves across preparations in these three different experimental realizations.

The *in vitro* experiments (Senseman, 1996, 1999) used an isolated preparation of the pond turtle, *Pseudemys scripta*, in which the brain and the attached eyes were surgically removed from the animal and were maintained in oxygenated Ringer's solution for up to 14 hours. This isolated eye-brain preparation is possible because diving turtles such as *P. scripta* have evolved an extraordinary resistance to anoxia as a defense against predation. To facilitate optical recording, the cortical sheet was freed at the midline and folded flat against the transparent bottom of the recording chamber. Since the lateral forebrain bundle that carries the geniculocortical afferents passes through the lateral wall of the cortex, this unfolding does not disturb the normal input from the eye.

To monitor cortical activity, the cortical sheet was stained with a voltage-sensitive dye (VSD) that alters its light absorbance at 700 nm in a rapid and linear manner with changes in the intracellular membrane potential of the stained cortical neurons. The preparation is trans-illuminated and the transmitted light collected by a 4X microscope objective and focused on to the surface of a 464-element silicon photodiode array to form a real image. At this magnification, each individual photodiode element records the algebraic summation of all the membrane potential taking place in a 300 μm × 300 μm × 700

μm volume of cortical tissue containing 600-700 spiny pyramidal cells and a smaller number of aspiny inhibitory interneurons. Collectively, this array of independent photodiode elements can be considered as a very fast video camera ($\leq$ 1 ms/frame), albeit one with moderately low spatial resolution. In these *in vitro* experiments, the photodiode array recorded "movies" of the VSD cortical images that captured changes in electrical activity evoked by stimulating the eye with diffuse light flashes.

In the *in vivo* experiments (Prechtl, et al., 1997) the surface of the brain was exposed by a craniotomy, and partially deafferented by sectioning the spinal cord. The cortical tissue was stained with a fluorescent voltage-sensitive dye injected into the cerebral spinal fluid. An epi-illumination system was used to excite the fluorescent dye while a 4X microscope objective focused the fluorescent VSD image on to a 464-element silicon photodiode array similar to the one used in the *in vitro* experiments. However, instead of using diffuse light flashes, the visual stimuli in the *in vivo* experiments were a looming white ball, trains of light flashes from a light emitting diode (LED) and sustained LED light pulses.

The numerical simulations used a physiologically-based model of the turtle visual cortex developed by Nenadic et al. (2002a, 2002b). Compartmental models of the four primary neuronal types (lateral pyramidal cells, medial pyramidal cells, stellate cells, and horizontal cells) were developed based on measured parameters. The connectivities of the cells were also based on measured densities. The cortex was driven by a linear array of lateral geniculate cells (LGN). The stimuli consisted of voltage applied to small patches of LGN cells for 50 ms. These patches should not be confused with the spot stimulation used for the *in vitro* experiments. The model patches correspond to an artificial stimulus applied directly at the boundary of the cortex, rather than to spots presented to the retina and propagated along the visual pathway.

Although the three experimental setups and stimulus presentations are very different, the responses in all three cases share common features. In each preparation, the response wave propagates in the rostral$\rightarrow$caudal direction and may undergo reflections as it reaches the caudal limits. This paper examines a derivative relationship among the modes that is found in all three preparations. The next

section of the paper introduces the notion of "derived modes". Section 3 compares the derived modes in the three cases. Section 4 discusses the comparison.

2. Duality and derived modes in KL decomposition

For signals that are sampled at discrete points in space and time, the measured response $\mathbf{U} = (u_{x,t})$ can be collected in an $L \times N$ matrix where $x = 1..L$ and $t = 1..N$ represent the sample numbers in space and time, respectively. The discrete proper orthogonal decomposition of $\mathbf{U}$ is:

$$\mathbf{U} = \sum_{k=1}^{r} \alpha_k \varphi^k (\psi^k)^T \qquad (1)$$

where r is the rank of $\mathbf{U}$, the φ^k's are $L \times 1$ vectors representing spatial basis functions, and the ψ^k's are $N \times 1$ vectors representing temporal basis functions. φ^k satisfies the eigenfunction relationship $\mathbf{R}\varphi^k = \lambda_k \varphi^k$ where $\mathbf{R} = \mathbf{U}\mathbf{U}^T$.

The proper orthogonal decomposition is equivalent to the Karhunen-Loeve decomposition (Aubrey,1991). Formally, KL decomposition is a statistical procedure applied to a random variable $\mathbf{u}^i$. KL finds the eigenvectors of the expected value of $\mathbf{u}^i(\mathbf{u}^i)^T$. Suppose that $\mathbf{u}^i$ represents a time sample of a spatial function. The expected value $E(\mathbf{u}^i(\mathbf{u}^i)^T)$ can be estimated as $\frac{1}{N}\sum_{i=1}^{N}\mathbf{u}^i(\mathbf{u}^i)^T$ which is $\frac{1}{N}\mathbf{U}\mathbf{U}^T = \frac{1}{N}\mathbf{R}$. Thus, although KL decomposition is a statistical procedure and proper orthogonal expansion is an algebraic one, the estimated orthogonal eigenvectors that result from KL decomposition are the same as the ones produced by proper orthogonal expansion.

Because $\mathbf{R}$ is a real nonnegative symmetric matrix of rank r, it has r real non-negative eigenvalues: $\lambda_1 \geq \lambda_2 \geq \ldots \geq \lambda_r \geq 0$. The eigenvectors corresponding to the positive eigenvalues are orthogonal, hence the temporal basis function ψ^j can be obtained by left multiplying Eq. (1) by the transpose of φ^j:

$$(\varphi^j)^T \mathbf{U} = \sum_{k=1}^{r} \alpha_k (\varphi^j)^T \varphi^k (\psi^k)^T = \sum_{k=1}^{r} \alpha_k \delta_{j,k} (\psi^k)^T = \alpha_j (\psi^j)^T$$

Taking the transpose of this equation and dividing by α_j gives:

$$\psi^j = \alpha_j^{-1} \mathbf{U}^T \varphi^j \qquad (2)$$

The ψ^j satisfy an eigenvalue equation $\mathbf{C}\psi^j = \lambda_j \psi^j$ where $\mathbf{C} = \mathbf{U}^T\mathbf{U}$ and the λ_j are the same eigenvalues as for $\mathbf{R}$ provided that $\lambda_j = \alpha_j^2$. Because $\mathbf{C}$ is a real, nonnegative symmetric matrix, the ψ^j's are orthogonal. The φ^j's can be recovered by multiplying Eq. (1) by ψ^j:

$$\mathbf{U}\psi^j = \sum_{k=1}^{r} \alpha_k \varphi^k (\psi^k)^T \psi^j = \sum_{k=1}^{r} \alpha_k \varphi^k \delta_{k,j} = \alpha_j (\varphi^j)$$

or:

$$\varphi^j = \alpha_j^{-1} \mathbf{U}\psi^j \qquad (3)$$

The *duality relationships* of Eq. (2) and Eq. (3) show that φ^j and ψ^j are duals of each other in the sense that one can be obtained from the other by projection on the original data set. These duality relationships are well-known and have previously been exploited to reduce the computational complexity of KL decomposition. One can choose to solve the eigenvalue problem either for the φ^j or for the ψ^j and use duality to get the other set. $\mathbf{R}$ is an $L \times L$ matrix, while $\mathbf{C}$ is an $N \times N$ matrix. If there are fewer time snapshots (N) than spatial points (L), it is more efficient to find the ψ^j's first. This observation is the basis of the method of snapshots proposed by Sirovich and Everson (1992).

In this paper, we exploit the duality relationship in a slightly different context. We have observed that the time derivatives $\frac{\partial \psi^p}{\partial t}$ seem to be related to ψ^q for certain *p* and *q*. We obtain *derived spatial basis functions* by assuming that the $\frac{\partial \psi^p}{\partial t}$ are temporal modes and using relationship (3). We then examine how the derived spatial modes are related to the spatial modes obtained from the original KL

decomposition. We denote the derived spatial basis function derived by projecting the time derivative of ψ^j by $(\varphi^j)' = \alpha_j^{-1}\mathbf{U}\frac{\partial \psi^j}{\partial t}$. Higher-order derived basis functions may also be calculated.

Results

We applied KL decomposition to the visual response in the three realizations of the turtle cortex (*in vitro*, *in vivo* and model) considered in this paper. As described in Senseman and Robbins (1999, 2002), we obtained a common or global spatial basis for each preparation by concatentating the responses for all of the stimuli and performing a KL decomposition on the result. We refer to this concatenation as the global KL decomposition. It should be noted that global decomposition is not equivalent to averaging trials before performing KL decomposition. Rather, it is a way to create a common basis so that the results obtained in different experimental trials can be directly compared.

While the details of the response differed quantitatively, the global KL decomposition in all three realizations gave a low-dimensional modal representation dominated by a large unimodal basis function. Other modes are distinguishable by the number of relative maxima and minima aligned with the major and minor axes of the largest modes. Senseman and Robbins (1999, 2002) used a modal numbering scheme for the *in vitro* preparation based on the observed alignment, with $M_{1,1}$ representing the largest mode and $M_{1,2}$ representing a mode with a single maximum and minimum separated by a line aligned along the minor axis of mode $M_{1,1}$. Furthermore, the time derivative of the projection of the data set on $M_{1,1}$ appeared to be highly correlated with projection of the data set on $M_{1,2}$. Because of this relationship, we investigated how closely $(M_{1,1})'$, the basis function derived from the time derivative of the projection on $M_{1,1}$ compared with $M_{1,1}$ in the three realizations of the turtle cortex. The results are shown in Figures 1 and 2.

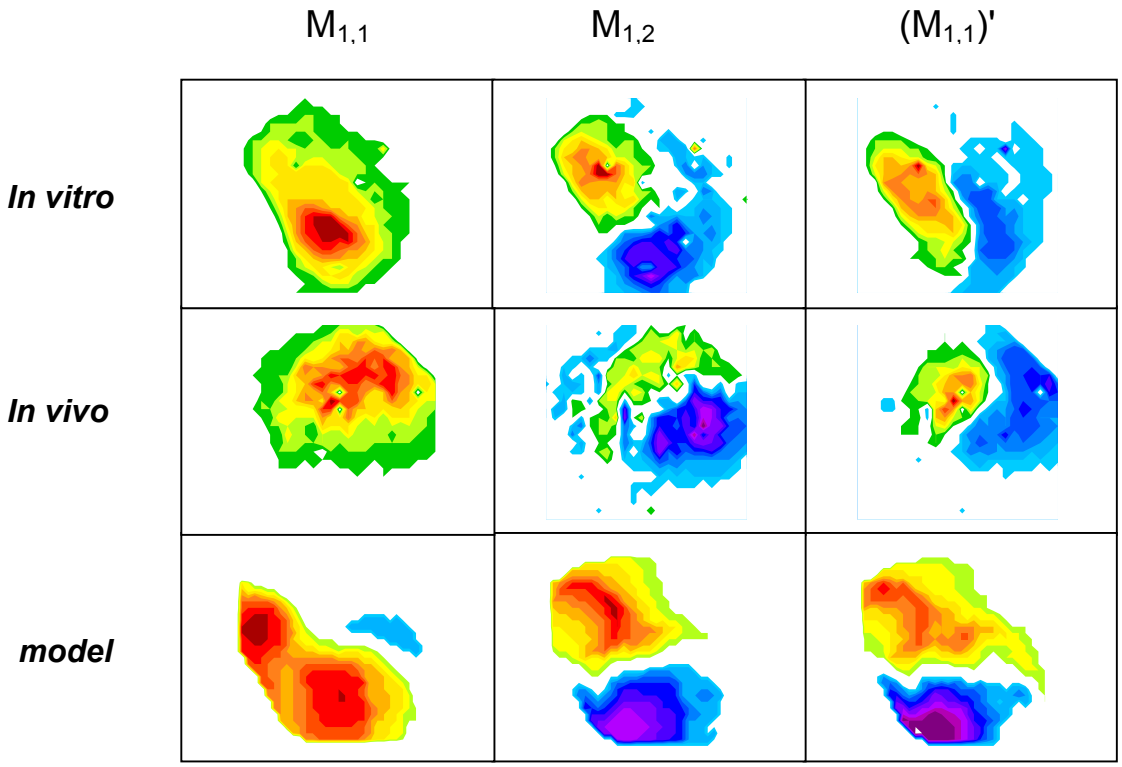

Fig. 1: A comparison of $M_{1,1}$, $M_{1,2}$ and $(M_{1,1})'$ for the three realizations of the turtle cortex.

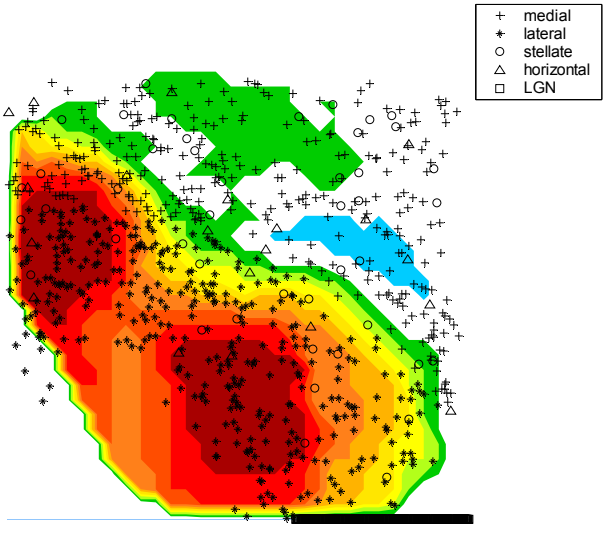

Fig. 2: The location of the neurons overlaid on $M_{1,1}$ for the model.

Discussion

Fig. 1 shows that there is a structural similarity in the modes and the derived modes in the three realizations of the turtle cortex, indicating a structural similarity in the waves that are generated in the three cases. It should be noted that the time courses of the projections on these modes differs significantly for different stimuli as would be expected in a system that has a modal expansion. Finding structural cues can be a guide to verifying that a model accurately portrays the behavior of the real system.

The modal notation is used because, while $M_{1,1}$ always corresponds to the largest KL mode, φ^1, the $M_{1,2}$ mode corresponds to φ^2 for the model, and mode φ^3 for the *in vitro* and *in vivo* data. The *in vivo* data has a large, low-frequency component, unrelated to the visual stimulation, that appears in φ^2 . Also, all of the realizations show a high frequency deviation from the base correlated behavior. Prior to examining the model data, we attributed this high-frequency component to experimental noise. The KL modes calculated before filtering or after filtering are virtually identical, but the projections calculated from unfiltered data must be filtered before derivatives can be calculated. For the data displayed in this paper, unfiltered data sets were used for the KL calculation. The projections were then filtered at 40 Hz before differentiation.

The KL decomposition for the model was performed by forming a vector of the voltages of the pyramidal cells. Once the spatial basis functions were obtained, linear interpolation was used with the Matlab contouring functions for display. However, there was no significant difference in the results, if the pyramidal cell voltages were first extrapolated to a square grid and KL decomposition was performed. This is noteworthy, because in the *in vitro* and *in vivo*

experiments, the photodiode array elements are measuring an average response. Fig. 2 shows the relationship of the neurons to the interpolation of the largest spatial basis function.

A derivative relationship among the projections would not be unexpected for a system that is described by a low-dimensional nonlinear differential equation. A well-known result from elementary differential equations (e.g., Boyce and DiPrima, 1965) is that a higher order differential equation for $y(t)$ can be converted to a system of first order differential equations by introducing dependent variables for the derivatives of y. Moreover, for systems that are described by partial differential equations, the spatial KL modes are the *linearized* normal modes (Breuer and Sirovich, 1991). When the model of a physical system is known, the spatial KL modes can be projected onto the model equations using Galerkin techniques to derive a simplified nonlinear ordinary differential equation (ODE) model of the physical system under investigation (Rodriguez and Sirovich, 1990). The results of this work suggest that such an ODE model of the turtle cortex response does exist and the KL modes may allow an empirical investigation of some aspects of its structure.

Acknowledgements

We thank L. Cohen for the generous donation of the data acquisition software and L. Cohen, D. Kleinfeld and P. Mitra for permission to use their *in vivo* data sets. We are also grateful to P. Ulinski, B. Ghosh and Z. Nenadic for their collaboration and for allowing us to use their model of the turtle cortex. This work was supported by the NIH (G12 RR13646), the NSF (ACI-9721348), the ONR (N00014-97-0029) and the UTSA Office of the Provost.

References

Aubry N, Guyonnet R, Lima R. Spatiotemporal analysis of complex signals: theory and applications. J Statistical Physics 64:683-739, 1991.

Boyce W, DiPrima R. Elementary Differential Equations and Boundary Value Problems. John Wiley & Sons Inc, 1965.

Breuer KS, Sirovich L. The use of the Karhunen–Loéve procedure for the calculation of linear eigenfunctions. J. Comput. Physics 96:277-296, 1991.

Nenadic Z, Ghosh BK, Ulinski PS. Spatiotemporal dynamics in a model of turtle visual cortex. Neurocomputing, 32-33: 479-486, 2000.

Nenadic Z, Ghosh BK, Ulinski PS. Modeling and estimation problems in the turtle visual cortex. IEEE Trans Biomed. Eng. in press.

Nenadic Z, Ghosh BK, Ulinski PS. Propagating waves in visual cortex: A large-scale model of turtle visual cortex. Neurocomputing, in press.

Prechtl JC. Visual motion induces synchronous oscillations in turtle visual cortex. PNAS 91:12467–12471, 1994.

Prechtl JC, Cohen LB, Pesaran B, Mitra PP, Kleinfeld D. Visual stimuli induce waves of electrical activity in turtle cortex. PNAS 94:7621-7626, 1997.

Prechtl JC, Bullock TH, Kleinfeld D. Direct evidence for local oscillatory current sources and intracortical phase gradients in turtle visual cortex. PNAS 97:877-882, 2000.

Robbins KA, Senseman DM. Visualizing differences in movies of cortical activity. IEEE Visualization ’98 217-224, 1998.

Rodriguez J, Sirovich L. Low dimensional dynamics for the complex Ginzburg-Landau equation. Physica D 43:77-86, 1990.

Senseman DM. Correspondence between visually evoked voltage-sensitive dye signals and synaptic activity recorded in cortical pyramidal cells with intracellular microelectrodes. Vis Neurosci 13:963–977, 1996.

Senseman DM. Spatiotemporal structure of depolarization spread in cortical pyramidal cell populations evoked by diffuse retinal light flashes. Vis Neurosci 16:65–79, 1999.

Senseman DM, Robbins KA. Modal behavior of cortical neural networks during visual processing. J Neurosci 19:RC3, 1–7, 1999.

Sirovich L, Everson R. Management and analysis of large scientific datasets. Intl. J of Supercomputer Applications 6(1):50–68, 1992.